MEDICAL SCIENCE MONITOR

LAB/IN VITRO RESEARCH

e-ISSN 1643-3750
© Med Sci Monit, 2015; 21: 3008-3015
DOI: 10.12659/MSM.894000

Received: 2015.03.03
Accepted: 2015.04.13
Published: 2015.10.06

MicroRNA-34a Promotes Hepatic Stellate Cell Activation via Targeting ACSL1

Authors' Contribution:
Study Design A
Data Collection B
Statistical Analysis C
Data Interpretation D
Manuscript Preparation E
Literature Search F
Funds Collection G

BE 1,2 Gangli Yan
CD 1 Binbin Li
DF 1,3 Xuan Xin
DF 1 Midie Xu
CF 4,5 Guoqing Ji
AEG 1 Hongyu Yu

1 Department of Pathology, Changzheng Hospital, The Second Military Medical University, Shanghai, P.R. China
2 Department of Neurology, The No. 161 People's Liberation Army (PLA) Hospital, Wuhan, Hubei, P.R. China
3 Department of Pathology, The General Hospital of the Jinan Military Command, Jinan, Shandong, P.R. China
4 State Key Laboratory of Genetic Engineering, Institute of Genetics, School of Life Sciences, Fudan University, Shanghai, P.R. China
5 Institutes of Biomedical Sciences, Fudan University, Shanghai, P.R. China

Corresponding Author: Hongyu Yu, e-mail: HongyuYu1234@163.com
Source of support: Departmental sources

Background: The incidence of liver fibrosis remains high due to the lack of effective therapies. Our previous work found that microRNA (miR)-34a expression was increased, while acy1-CoA synthetase long-chain family member1 (ACSL1) was decreased, in a dimethylnitrosamine (DNS)-induced hepatic fibrosis rat model. We hypothesized that miR-34a may play a role in the process of hepatic fibrosis by targeting ACSL1.

Material/Methods: From days 2 to 14, cultured primary hepatic stellate cells (HSCs) underwent cell morphology, immunocytochemical staining, and quantitative reverse transcription PCR (RT-qPCR) for alpha smooth muscle actin (α-SMA), desmin, rno-miR-34a, and ACSL1 expression. Wild-type and mutant luciferase reporter plasmids were constructed according to the predicted miR-34a binding site on the 3'-untranslated region (UTR) of the ACSL1 mRNA and then transfected into HEK293 cells. rno-miR-34a was silenced in HSCs to confirm that rno-miR-34a negatively regulates ACSL1 expression. mRNA and protein expression of α-SMA, type I collagen, and desmin were assayed in miR-34a-silenced HSCs.

Results: HSCs were deemed quiescent during the first 3 days and activated after 10 days. rno-miR-34a expression increased, and ACSL1 expression decreased, from day 2 to 7 to 14. rno-miR-34a was shown to specifically bind to the 3'-UTR of ACSL1. miR-34a-silenced HSCs showed higher ACSL1and lower α-SMA, type I collagen, and desmin expression than that of matching negative controls and non-transfected cells.

Conclusions: miR-34a appears to play an important role in the process of liver fibrosis by targeting ACSL1 and may show promise as a therapeutic molecular target for hepatic fibrosis.

MeSH Keywords: Hepatic Stellate Cells • Liver Cirrhosis • MicroRNAs

Full-text PDF: http://www.medscimonit.com/abstract/index/idArt/894000

2741 — 7 36

Indexed in: [Current Contents/Clinical Medicine] [SCI Expanded] [ISI Alerting System] [ISI Journals Master List] [Index Medicus/MEDLINE] [EMBASE/Excerpta Medica] [Chemical Abstracts/CAS] [Index Copernicus]

Background

Liver fibrosis is a key pathological process underlying a variety of chronic liver diseases, including viral hepatitis, alcoholic fatty liver disease, and cholestatic liver disease [1–4]. Although liver fibrosis is not malignant in and of itself, the process can destroy normal tissue structure and function and can gradually develop into cirrhosis, and eventually liver cancer. Hepatic stellate cells (HSCs) are vitamin A-storing pericytes found in the space of Disse [5]. Activation and proliferation of HSCs is pivotal to the development of liver fibrosis [4,6,7]. HSCs are activated to myofibroblasts (MFs) through the epithelial-to-mesenchymal transition (EMT) and secretion of extracellular matrix (ECM) through autocrine and paracrine processes. In addition, HSCs secrete tissue inhibitors of matrix metalloproteinases (TIMPs), which reduce ECM degradation. When ECM synthesis outpaces ECM degradation, the resulting superabundant ECM deposition can lead to liver fibrosis [8,9]. However, the molecular mechanism(s) underlying liver fibrosis is not yet fully understood.

As an epigenetic regulatory mechanism, microRNAs (miRNA, miR) have become increasingly important in the process of liver fibrosis [10–12]. In our previous study that applied chip screening technology, a variety of miRNAs were found to be differentially expressed in a dimethylnitrosamine (DNS)-induced hepatic fibrosis rat model, including miR-214, miR-199a-3p, miR-324-5p, miR-878, miR-7a, and miR-34a; in particular, miR-34a displayed significantly increased levels and was positively correlated with liver fibrosis [13]. Simultaneously, from our bioinformatics analysis, we discovered that miR-34a may target acy1-CoA synthetase long-chain family member 1 (ACSL1). Previous reviews have discussed ACSL1's important role as a channel for fatty acid and lipid metabolism, a process which has been previously associated with liver fibrosis [14–16].

On the basis of these previous findings, we hypothesized that miR-34a may play an important role in the process of hepatic fibrosis by targeting ACSL1. In the present study, we verified that rno-miR-34a is significantly upregulated with the activation of primary HSCs and confirmed that ACSL1 is the target gene of rno-miR-34a using a luciferase reporter system in the tool cell line 293T. In addition, we found that rno-miR-34a regulates the deposition of ECM proteins, including type I collagen, desmin, and alpha smooth muscle actin (α-SMA) via its interaction with ACSL1's 3'-UTR. These results suggest that silencing miR-34a in HSCs may be applied as a future therapeutic strategy for liver fibrosis.

Material and Methods

HSC isolation and culture

Primary rat HSCs were isolated from male Sprague-Dawley rats (300–400 g) by *in situ* liver pronase/collagenase perfusion and 18% Nycodenz density gradient centrifugation according to Kawada et al.'s method [17,18]. Briefly, under ethyl ether anesthesia, the rat liver was perfused at 10 ml/min via the portal vein with Gey's balanced salt solution (GBSS, pH 7.3) for 10 min at 37°C and then with GBSS containing 0.08% pronase E and 0.04% collagenase for 30 min at 37°C. Post-perfusion, the rat liver was digested in GBSS containing 0.05% pronase E, 0.05% collagenase, and 20 μg/ml of deoxyribonuclease for 30 min at 37°C and then filtered through a 150-mm mesh. After 18% Nycodenz cushion centrifugation at 1400×g for 15 min at 4°C, the HSC-enriched fraction was obtained from the upper white-colored layer. Cells were washed by centrifugation at 400×g for 10 min at 4°C and then cultured on uncoated plastic dishes in DMEM (Thermo, China) supplemented with 10% fetal bovine serum (FBS, Gibco, USA). HSCs were morphologically identified by their typical star-like configuration. Cell viability and purity were more than 95%, which was confirmed by Trypan Blue staining and auto-fluorescence.

Both HSCs and the human embryonic kidney tool cell line 293T (ATCC, USA) were cultured in DMEM (Thermo, China) supplemented with 10% FBS (Gibco, USA), 100 μg/ml streptomycin, and 100 U/ml penicillin. Cells were grown in a 37°C incubator at 5% CO_2.The medium was changed every two days, and cells were passaged upon reaching 70-80% confluence.

Immunocytochemical staining

HSCs were rinsed in PBS three times for 3 min each. The cells were fixed for 10 min in 4% formaldehyde and then permeabilized in 0.5% Triton X-100 in PBS for 20 min at room temperature. Slides were dipped in PBS three times for 3 min each. A blocking solution consisting of PBS (pH 7.5) with 1% normal goat serum was added drop-wise on each slide and kept at room temperature for 30 min. Then, the excess blocking solution was blotted off with absorbent paper. Slides were treated with diluted primary antibody (anti-α-SMA, 1:100; anti-desmin, 1:100) and placed in a wet box at 4°C for overnight incubation.

After overnight incubation, fluorescent secondary antibodies were applied in a dark environment. Slides were dipped in PBST three times for 3 min each. The excess secondary antibody was blotted off with absorbent paper, and slides were placed in a wet box at 20–37°C for 1 h of incubation. Slides were dipped in PBST three times for 3 min each. Nuclei were stained by application of DAPI stain in the dark for 5 min. Then, excess DAPI stain was washed away with PBST four times for

Indexed in: [Current Contents/Clinical Medicine] [SCI Expanded] [ISI Alerting System] [ISI Journals Master List] [Index Medicus/MEDLINE] [EMBASE/Excerpta Medica] [Chemical Abstracts/CAS] [Index Copernicus]

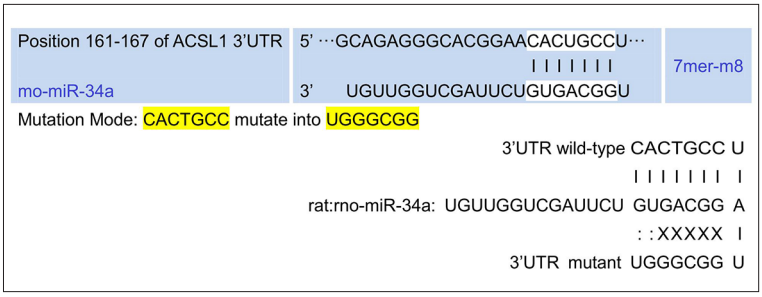

Supplementary Figure 1. Predicted binding site and mutated site construction.

5 min each. Slides were mounted with an anti-fluorescence quench reagent for fluorescent imaging.

Transfection

According to the phenotypic changes, HSCs were deemed quiescent on day 2 and then activated on day 14. HSCs were seeded onto six-well plates at a density of 4.5×10^5/well on day 14 and divided into three experimental groups: (i) the miR-34a-silenced group, (ii) the miR-22-silenced negative control (NC) group, and (iii) the non-transfected (NT) group. miR-22 was specifically chosen as the NC based on our previous findings in the same DMN-induced liver fibrosis model, which displayed no changes in miR-22 expression in rat HSCs by miRNA expression microarray analysis [13].

The miR-34a-silenced group was transfected with a rno-miR-34a silencing vector, and the NC group was transfected with a miRNA-22 silencing vector using lipofectamine2000 (Invitrogen, USA) according to the manufacturer's protocol. The rno-miR-34a silencing vector and miRNA-22 silencing vector were both purchased from the Ribo Company (Guangzhou, China). The adherent cells reached a 50% cell density the next day. Then, the mRNA/miRNA/protein was extracted from the cells for RT-PCR or Western Bolt analysis 48 h post-transfection.

RT-PCR and real-time RT-PCR

Total RNA was extracted using Trizol reagent (Invitrogen, USA). miRNA was reverse transcribed to cDNA with a specific stem-loop primer, and the mRNA was reversed transcribed to cDNA with Oligo dT Primer and Random 6 mers using a PrimeScript™ RT reagent kit (TaKaRa, Japan). Then, they were subjected to a RT reaction using SYBR Premix Ex Taq™ II (TaKaRa, Japan) in the ABI 7900HT Fast Real-time PCR System (Singapore) using the following gene-specific oligonucleotide primers: rno-miR-34a, forward-5'CTCGGATCCTTTCTCCCACAGCCTCTC and reverse-5'CGGAATTCTAGAGCAGCTCCCGAAGTCC; α-SMA, forward-5'TTCCTTCGTGACTACTGCTGAG and reverse-5'CAATGAAAGATGGCTGGAAGAG; desmin, forward-5'CAGCAGGTCCAGGTAGAGATG and reverse-5'GAGATGTTCTTAGCCGCAATG; type I collagen, forward-5'ATGTCTGGTTTGGAGAGAGCA and reverse-5'GAGGAGCAGGGACTTCTTGAG;GAPDH, forward-5'ACAGCAACAGGGTGGTGGAC and reverse-5'TTTGAGGGTGCAGCGAACTT. The relative amounts of miRNA and mRNA were normalized against U6 snRNA and GAPDH, respectively. The fold-changes for miRNA and mRNA expression were calculated by the $2^{-\Delta\Delta Ct}$ method.

Luciferase reporter assay

A luciferase reporter assay was used to verify whether rno-miR-34a directly binds to the 3'-UTR of ACSL1 in the HEK293T cell line. First, the 3'-UTR of ACSL1 fragments containing the predicted binding site for rno-miR-34a and a 3'-UTR-mutation were constructed (Supplementary Figure 1). Then, fragments were inserted into the 3'-end of the firefly-luciferase gene in the dual-luciferase target gene expression vector (Promega, USA). 293T cells were seeded onto a 96-well plate (2.5×10^4 cells per well) one day before transfection. When the cells reached a density of 70% the next day, the cells were transiently transfected with either the miR-34a-silenced (100 nm) or NC (100 nm) versions of each constructed plasmid. Firefly and Renilla relative luciferase activity was measured using the Dual-Luciferase Reporter Assay System (Promega, USA) 48 hours post-transfection according to the manufacturer's protocols.

Western blot analysis

HSCs were harvested and lysed into RIPA buffer on ice. The BCA method was used to measure protein concentration. Proteins were transferred to a polyvinylidene difluoride (PVDF) membrane after 10% (w/v) sodium dodecyl sulfate polyacrylamide gel electrophoresis (SDS-PAGE). Membranes were blocked for 2 h and then incubated with the following primary antibodies: anti-ACSL1 rabbit polyclonal antibody (Thermo), anti-type I collagen rabbit polyclonal antibody (ab34710), anti-α-SMA rabbit polyclonal antibody (ab5694), anti-desmin rabbit monoclonal antibody (ab32362), and anti-GAPDH rabbit monoclonal antibody (ab9485). This was followed by incubation with peroxidase-conjugated secondary antibodies (Abmart, China) for 60 minutes. Protein expression was then analyzed by Western blotting.

Statistical analysis

All experiments were performed in triplicate. All values are reported as means ± standard deviations (SDs). Student's *t*-test

Indexed in: [Current Contents/Clinical Medicine] [SCI Expanded] [ISI Alerting System] [ISI Journals Master List] [Index Medicus/MEDLINE] [EMBASE/Excerpta Medica] [Chemical Abstracts/CAS] [Index Copernicus]

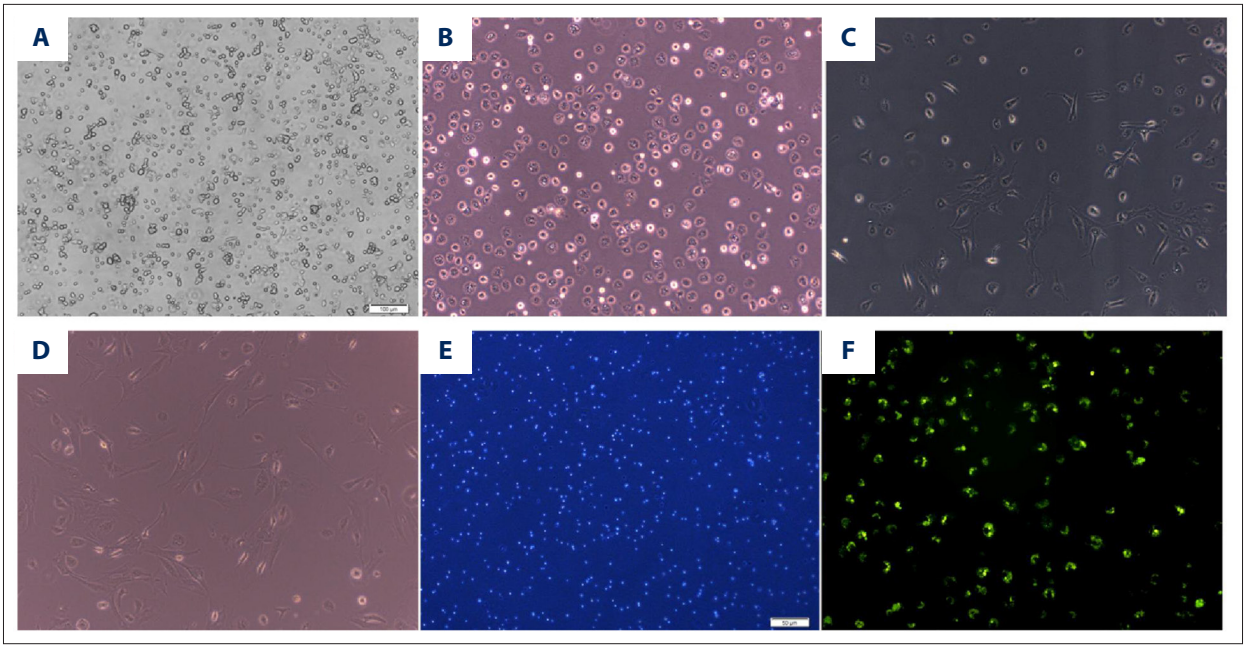

Figure 1. Identification and morphology of primary HSCs by light microscopy. (**A**) On day 1, HSCs were round and of uniform size and emitting strong blue-green auto-fluorescence under 327-nm UV wavelength stimulation (10×). (**B**) On day 2, HSCs were adherent by showing *in vitro* cell attachment and were round (or oval)-shaped (10×). (C) On day 7, the cell bodies extended outward (i.e., forming a drop-like appearance) with aggregate growth (10×). (**D**) On day 14, the cell bodies fully extended (i.e., dendritic cell-like appearance) (10×). (**E**) Trypan blue identification of cell viability (4×) revealed ~95% cell survival with dead cells showing dark blue dye exclusion and living cells showing colorless transparency. (**F**) HSCs emit yellow-green fluorescence under 328-nm UV wavelength stimulation (10×).

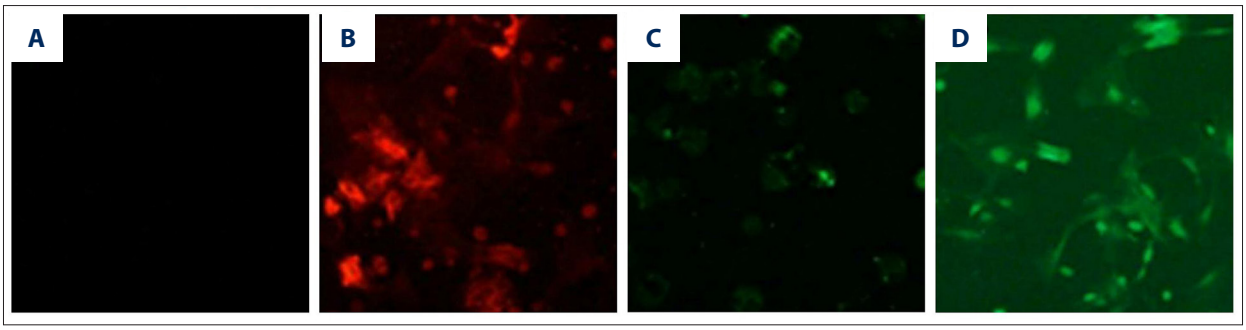

Figure 2. Immunocytochemical staining of primary HSCs. (**A**) On day 2, α-SMA expression (staining green) was negative with DAPI-stained nuclei (staining blue) (20×). (**B**) On day 14, α-SMA expression (staining green) was positive with DAPI-stained nuclei (staining blue) (20×). (**C**) On day 2, cytoplasmic desmin expression (staining red) was slightly positive with DAPI-stained nuclei (staining blue) (20×). (**D**) On day 14, cytoplasmic desmin expression (staining red) was positive with DAPI-stained nuclei (staining blue) (20×).

was used for comparisons between two groups, and a one-way analysis of variance (ANOVA) test was used for multiple comparisons between three groups. Differences meeting a $p<0.05$ threshold were considered to be statistically significant. All analyses were performed using SPSS 17.0.

Results

Identification of quiescent and activated HSCs

The status of HSCs was detected in the primary cells during activation (Figure 1). Upon isolation from rats, the HSCs displayed a round morphology with a blue-green intrinsic auto-fluorescence under 327-nm UV wavelength stimulation. Under light microscopy on day 2, HSCs were adherent with a round

Indexed in: [Current Contents/Clinical Medicine] [SCI Expanded] [ISI Alerting System] [ISI Journals Master List] [Index Medicus/MEDLINE] [EMBASE/Excerpta Medica] [Chemical Abstracts/CAS] [Index Copernicus]

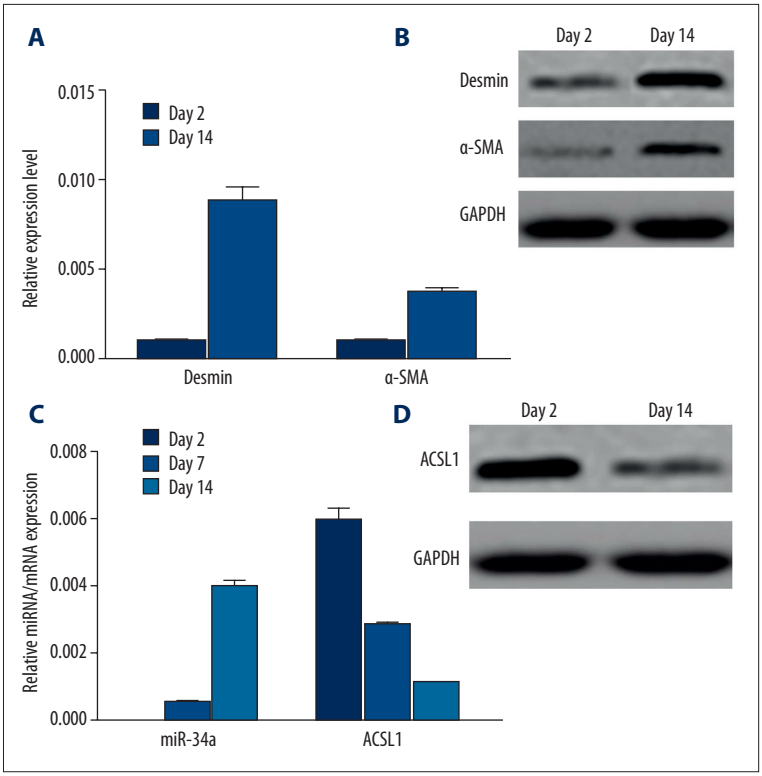

Figure 3. Desmin, α-SMA, miR-34a, and ACSL1 expression in HSCs. (**A**) miRNA expression of desmin and α-SMA ($p<0.05$). (**B**) Protein expression of desmin and α-SMA. (**C**) Significant rno-miR-34a upregulation and ACSL1 mRNA downregulation observed in activated HSCs ($p<0.05$). (**D**) ACSL1 protein expression was downregulated in activated HSCs at day 14 compared to quiescent HSCs at day 2.

or oval-shaped morphology. On day 7, the cell body extended outward, and on day 14, the cell bodies were fully extended, displaying a morphology similar to dendritic neurons. Based on these observations, HSCs were deemed quiescent during the first 3 days and activated after 10 days [19].

Immunocytochemical staining and RT-qPCR for α-SMA and desmin demonstrated the quiescent and activated phenotypes of HSCs on days 2 and 14, respectively (Figure 2). rno-miR-34a and ACSL1 expression were determined on days 2,7, and 14. rno-miR-34a and ACSL1 were expressed differently in quiescent and activated HSCs – rno-miR-34a was upregulated in activated cells, while ACSL1 was downregulated in activated cells (Figure 3).

MiR-34a and ACSL1 expression in primary HSCs at days 2 and 14

rno-miR-34a and ACSL1 expression were assessed in primary HSCs on days 2, 7, and 14. rno-miR-34a expression increased gradually from day 2 to day 7 to day 14, while ACSL expression decreased from day 2 to day 7 to day 14, which reveals that rno-miR-34a upregulation and ACSL1 downregulation are associated with HSC activation. Western blotting found that ACSL1 protein expression was downregulated in HSCs on day 14 compared to quiescent HSCs on day 2 (Figure 3).

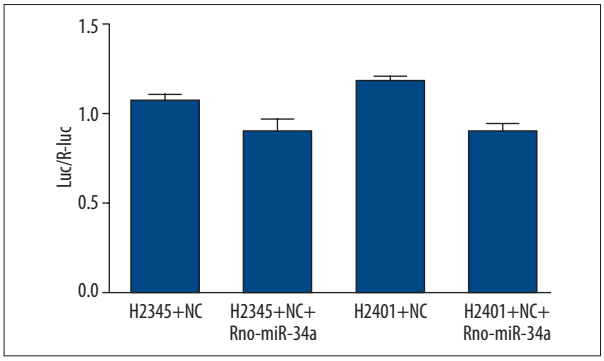

Supplementary Figure 2. Luciferase reporter activity. Luciferase reporter activity was raised in HEK293 cells transfected with wild-type (WT) constructive luciferase reporter plasmid ($p<0.05$). There were no changes in HEK293 cells transfected with the mutant (MUT) constructive luciferase reporter plasmid ($p<0.05$).

MiR-34a directly targets ACSL1

Our previous study found that ACSL1 may be a target of miR-34a, so here we constructed wild-type (WT) and mutant (MUT) luciferase reporter plasmids according to the predicted rno-miR-34a binding site on the 3'-UTR of the ACSL1 mRNA. Then, HEK293 cells were transfected with either the miR-34a-silenced or NC versions of each constructed plasmid. rno-miR-34a silencing significantly raised luciferase reporter activity in HEK293

Indexed in: [Current Contents/Clinical Medicine] [SCI Expanded] [ISI Alerting System] [ISI Journals Master List] [Index Medicus/MEDLINE] [EMBASE/Excerpta Medica] [Chemical Abstracts/CAS] [Index Copernicus]

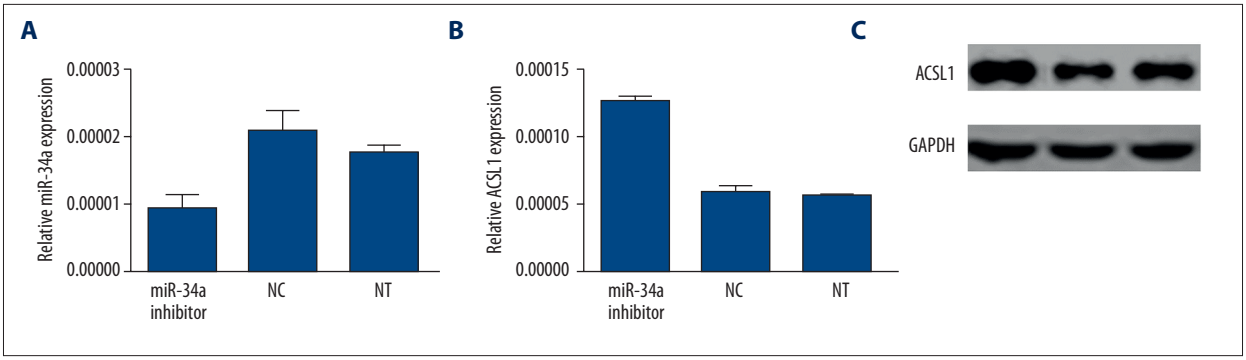

Figure 4. miR-34a and ACSL1 expression post-transfection. (**A**) rno-miR-34a expression in miR-34a-silenced HSCs was significantly lower than that of matching NC and NT cells ($p<0.05$), and there was no significant difference between NC and NT cells ($p>0.05$). (**B**) ACSL1 mRNA expression in miR-34a-silenced HSCs was significantly higher than that of matching NC and NT cells ($p<0.05$), and there was no significant difference between NC and NT cells ($p>0.05$). (**C**) ACSL1 protein expression in miR-34a-silenced HSCs was significantly higher than that of matching NC and NT cells, and there was no significant difference between NC and NT cells ($p>0.05$).

cells transfected with the WT constructive luciferase reporter plasmid ($p<0.05$). However, there were no changes in HEK293 cells transfected with the MUT constructive luciferase reporter plasmid ($p>0.05$; Supplementary Figure 2).The results indicate that rno-miR-34a specifically binds to the 3'-UTR of ACSL1.

MiR-34a negatively regulates ACSL1 mRNA and protein expression

To confirm that rno-miR-34a negatively regulates ACSL1 expression, rno-miR-34a and ACSL1 expression levels were examined in miR-34a-silenced HSCs as well as matching NC and NT cells. As expected, rno-miR-34a expression in miR-34a-silenced HSCs was significantly lower than that of the NC and NT cells ($p<0.05$), and there was no significant difference between NC and NT cells ($p>0.05$), implying that the miR-34a-silencing vector was successfully transfected into HSCs (Figure 4).

ACSL1 mRNA expression in miR-34a-silenced HSCs was significantly higher than that of NC and NT cells ($p<0.05$), and there was no significant difference between NC and NT cells ($p>0.05$; Figure 4B). Accordingly, Western blotting revealed that ACSL1 protein expression in miR-34a-silenced HSCs was significantly higher than that of NC and NT cells ($p<0.05$), and there was no significant difference between NC and NT cells ($p>0.05$; Figure 4C).These findings confirm that ACSL1 expression is negatively regulated by rno-miR-34a.

MiR-34a affects HSC activation

Finally, to explore the biological role of rno-miR-34a in HSC activation (if any), we assessed the effect of rno-miR-34a levels on ECM mRNA and protein expression in HSCs. The mRNA and protein expression of α-SMA, type I collagen, and desmin were examined in miR-34a-silenced HSCs as well as matching NC and NT cells. α-SMA, type I collagen, and desmin mRNA expression in miR-34a-silenced HSCs was lower than that of the NC and NT cells ($p<0.05$), and there was no significant difference between NC and NT cells ($p>0.05$; Figure 5A). Among the three ECM mRNAs, the change in type I collagen mRNA expression was most obvious. Similar results were found from the analogous protein expression experiments (Figure 5B).

Discussion

Hepatic fibrosis, which is an abnormal fibrotic hyperplasia caused by chronic hepatopathy, is characterized by excessive ECM deposition. ECM proteins – such as α-SMA, type I collagen, type IV collagen, and desmin – are excessively secreted by activated HSCs, which destroys the normal liver structure and eventually results in liver fibrosis. As HSC activation plays an important role in the course of liver fibrosis, the objective of the present study was to explore the pro-fibrotic role of miR-34a (if any) through its interaction with ACSL1.

MiRNAs are a class of small non-coding RNA containing about 18–22 nucleotides that regulate gene expression transcriptionally and post-transcriptionally [20,21]. Most miRNAs play multiple negative regulatory roles, such as transcript degradation and translational suppression. MiRNAs can specifically bind to the 3'-UTR of their target genes. According to recent studies, over 1000 miRNAs are encoded by the human genome [22], which may target up to 60% of mammalian mRNAs [23,24]. Different miRNA expression signatures have been found across various tissues and diseases, and miRNA-based therapeutic methods are still an active area of investigation [25–28].

Our previous research found multiple miRNAs were dysregulated in DMN-induced liver fibrosis rat model with some

Indexed in: [Current Contents/Clinical Medicine] [SCI Expanded] [ISI Alerting System] [ISI Journals Master List] [Index Medicus/MEDLINE] [EMBASE/Excerpta Medica] [Chemical Abstracts/CAS] [Index Copernicus]

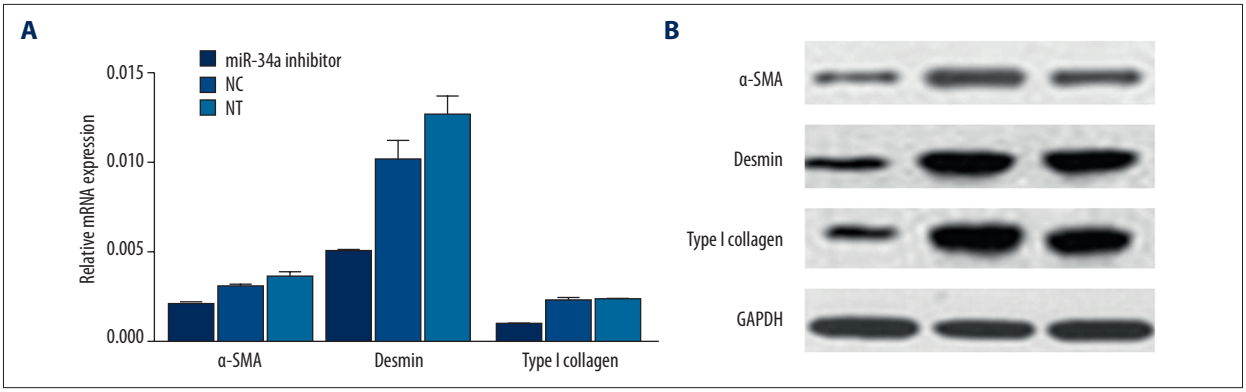

Figure 5. α-SMA, Type I collagen, and desmin expression post-transfection. (**A**) α-SMA, type I collagen, and desmin mRNA expression in miR-34a-silenced HSCs was significantly lower than that of matching NC and NT cells ($p<0.05$), and there was no significant difference between NC and NT cells ($p>0.05$). (**B**) α-SMA, type I collagen, and desmin protein expression in miR-34a-silenced HSCs was significantly lower than that of matching NC and NT cells ($p<0.05$), and there was no significant difference between NC and NT cells ($p>0.05$).

upregulated miRNAs, such as miR-34a, being associated with lipid metabolism [13]. In this study, we revealed that rno-miR-34a expression was significantly increased, while ACSL1 expression was decreased, in activated primary HSCs relative to quiescent HSCs. When rno-miR-34a expression was silenced in activated HSCs, ACSL1 mRNA and protein expression were both significantly increased.

ACSL is a family of enzymes that use long-chain fatty acids (LCFAs), ATP, and CoA to synthesize acyl-CoA derivatives, a process which is required for fatty acids to enter into lipid pools, β-oxidation, and other biological effects of fatty acids [16]. The five ACSL isoforms that are expressed in mammals (ACSL1, ACSL3, ACSL4, ACLS5, and ACSL6) are encoded by a diverse set of genes [29,30] and possess unique biological functions which are cell type- and content-dependent on the availability of different fatty acid substrates under different conditions [31]. ACSL1 has been previously detected in adipocytes [32], cardiomyocytes [33], and hepatocytes [34], and our previous work has detected ACSL1 expression in HSCs [13]. To determine whether ACSL1 is a direct target of rno-miR-34a, here we used a luciferase reporter assay to analyze rno-miR-34a function on predicted binding sites. The data revealed that rno-miR-34a could effectively bind to the WT sequence, but not to the MUT sequence, confirming that ACSL1 is a functional target of rno-miR-34a. Furthermore, we assessed the biological effects of rno-miR-34a's targeting of ACSL1, through analyzing the expression of α-SMA, type I collagen, and desmin. We found that α-SMA, type I collagen, and desmin expression decreased after rno-miR-34a silencing, indicating that rno-miR-34a downregulation enables culture-activated HSCs to transform to the more quiescent HSCs phenotype.

We hypothesize that miR-34a silencing disinhibits ACSL1 expression through preventing miR-34a's binding to the 3'-UTR of the ACSL1 mRNA. This miR-34a silencing increases ACSL1 expression, thereby activating LCFAs to form acyl-CoAs and promoting lipogenesis by increasing fatty acid uptake into hepatic cells [13,35]. As induction of the transcription factors PPARα, SREBP-1, and C/EBPα has been shown to lead to lipid accumulation (lipogenesis) and inhibition of HSC activation [36], the increase in ACSL1 expression by miR-34a silencing may serve to promote HSC lipogenesis, thereby restoring healthy HSC lipid metabolism and inhibiting HSC activation. This transformation from an activated HSC phenotype to a more quiescent phenotype can aid in preventing the progression of liver fibrosis. Further detailed studies on HSCs should be performed to verify this hypothesis.

Conclusions

We found miR-34a is upregulated in activated HSCs via targeting of ACSL1, which presents a new therapeutic target opportunity for liver fibrosis. However, this study also raises some complex questions, such as: what are the upstream stimulators of miR-34a expression? what is the precise intracellular localization of ACSL1?, and how does ACSL1's downstream signaling pathway regulate liver fibrotic activity? Further *in vitro* studies are needed to address these open questions.

Acknowledgments

The authors thank Shanghai Obio Technology Co., Ltd. for their technical assistance.

Indexed in: [Current Contents/Clinical Medicine] [SCI Expanded] [ISI Alerting System] [ISI Journals Master List] [Index Medicus/MEDLINE] [EMBASE/Excerpta Medica] [Chemical Abstracts/CAS] [Index Copernicus]

References:

1. Alcolado R, Iredale P: Pathogenesis of liver fibrosis. Studies, 1997; 50: 51
2. Friedman SL: Evolving challenges in hepatic fibrosis. Nat Rev Gastroenterol Hepatol, 2010; 7: 425–36
3. Wang XW, Heegaard NH, Ørum H: MicroRNAs in liver disease. Gastroenterology, 2012; 142: 1431–43
4. Lu P, Liu H, Yin H, Yang L: Expression of angiotensinogen during hepatic fibrogenesis and its effect on hepatic stellate cells. Am J Case Rep, 2011; 17: 248–56
5. Qu Y, Chen W-H, Zong L et al: 18alpha-Glycyrrhizin induces apoptosis and suppresses activation of rat hepatic stellate cells. Med Sci Monit Basic Res, 2011; 18: 24–32
6. Friedman SL: Molecular regulation of hepatic fibrosis, an integrated cellular response to tissue injury. J Biol Chem, 2000; 275: 2247–50
7. Wu J, Zern MA: Hepatic stellate cells: a target for the treatment of liver fibrosis. J Gastroenterol, 2000; 35: 665–72
8. Veidal SS, Nielsen MJ, Leeming DJ, Karsdal MA: Phosphodiesterase inhibition mediates matrix metalloproteinase activity and the level of collagen degradation fragments in a liver fibrosis *ex vivo* rat model. BMC Res Notes, 2012; 5: 686
9. Mòdol T, Brice N, Ruiz de Galarreta M et al: Fibronectin peptides as potential regulators of hepatic fibrosis through apoptosis of hepatic stellate cells. J Cell Physiol, 2015; 230: 546–53
10. Haybaeck J, Zeller N, Heikenwalder M: The parallel universe: microRNAs and their role in chronic hepatitis, liver tissue damage and hepatocarcinogenesis. Swiss Med Wkly, 2011; 141: w13287
11. Vettori S, Gay S, Distler O: Role of microRNAs in fibrosis. Open Rheumatol J, 2012; 6: 130–39
12. Zhang J-w, Li Y, Zeng X-C et al: miR-630 overexpression in hepatocellular carcinoma tissues is positively correlated with alpha-fetoprotein. Med Sci Monit, 2015; 21: 667–73
13. Li WQ, Chen C, Xu MD et al: The rno-miR-34 family is upregulated and targets ACSL1 in dimethylnitrosamine-induced hepatic fibrosis in rats. FEBS J, 2011; 278: 1522–32
14. Parkes HA, Preston E, Wilks D et al: Overexpression of acyl-CoA synthetase-1 increases lipid deposition in hepatic (HepG2) cells and rodent liver *in vivo*. Am J Physiol Endocrinol Metab, 2006; 291: E737–44
15. Soupene E, Kuypers FA: Mammalian long-chain acyl-CoA synthetases. Exp Biol Med, 2008; 233: 507–21
16. Ellis JM, Frahm JL, Li LO, Coleman RA: Acyl-coenzyme A synthetases in metabolic control. Curr Opin Lipidol, 2010; 21: 212–17
17. Kojima-Yuasa A, Ohkita T, Yukami K et al: Involvement of intracellular glutathione in zinc deficiency-induced activation of hepatic stellate cells. Chem Biol Interact, 2003; 146: 89–99
18. Kawada N, Tran-Thi TA, Klein H, Decker K: The contraction of hepatic stellate (Ito) cells stimulated with vasoactive substances. Eur J Biochem, 1993; 213: 815–23
19. Ji J, Zhang J, Huang G et al: Over-expressed microRNA-27a and 27b influence fat accumulation and cell proliferation during rat hepatic stellate cell activation. FEBS Lett, 2009; 583: 759–66
20. Chen K, Rajewsky N: The evolution of gene regulation by transcription factors and microRNAs. Nat Rev Genet, 2007; 8: 93–103
21. Tang G, Shen X, Lv K et al: Different normalization strategies might cause inconsistent variation in circulating microRNAs in patients with hepatocellular carcinoma. Med Sci Monit, 2015; 21: 617–24
22. Bartel DP: MicroRNAs: target recognition and regulatory functions. Cell, 2009; 136: 215–33
23. Lewis BP, Burge CB, Bartel DP: Conserved seed pairing, often flanked by adenosines, indicates that thousands of human genes are microRNA targets. Cell, 2005; 120: 15–20
24. Friedman RC, Farh KK-H, Burge CB, Bartel DP: Most mammalian mRNAs are conserved targets of microRNAs. Genome Res, 2009; 19: 92–105
25. Lagos-Quintana M, Rauhut R, Yalcin A, Meyer J et al: Identification of tissue-specific microRNAs from mouse. Curr Biol, 2002; 12: 735–39
26. Trang P, Weidhaas J, Slack F: MicroRNAs as potential cancer therapeutics. Oncogene, 2008; 27: S52–57
27. Li C, Feng Y, Coukos G, Zhang L: Therapeutic microRNA strategies in human cancer. AAPS J, 2009; 11: 747–57
28. Fasanaro P, Greco S, Ivan M et al: microRNA: emerging therapeutic targets in acute ischemic diseases. Pharmacol Ther, 2010; 125: 92–104
29. Sandoval A, Fraisl P, Arias-Barrau E et al: Fatty acid transport and activation and the expression patterns of genes involved in fatty acid trafficking. Arch Biochem Biophys, 2008; 477: 363–71
30. Li X, Gonzalez O, Shen X et al: Endothelial acyl-CoA synthetase 1 is not required for inflammatory and apoptotic effects of a saturated fatty acid-rich environment. Arterioscler Thromb Vasc Biol, 2013; 33: 232–40
31. Umlauf E, Csaszar E, Moertelmaier M et al: Association of stomatin with lipid bodies. J Biol Chem, 2004; 279: 23699–709
32. Kang M-J, Fujino T, Sasano H et al: A novel arachidonate-preferring acyl-CoA synthetase is present in steroidogenic cells of the rat adrenal, ovary, and testis. Proc Natl Acad Sci USA, 1997; 94: 2880–84
33. Ellis JM, Mentock SM, DePetrillo MA et al: Mouse cardiac acyl coenzyme a synthetase 1 deficiency impairs fatty acid oxidation and induces cardiac hypertrophy. Mol Cell Biol, 2011; 31: 1252–62
34. Li LO, Ellis JM, Paich HA et al: Liver-specific loss of long chain acyl-CoA synthetase-1 decreases triacylglycerol synthesis and β-oxidation and alters phospholipid fatty acid composition. J Biol Chem, 2009; 284: 27816–26
35. Cui M, Wang Y, Sun B et al: MiR-205 modulates abnormal lipid metabolism of hepatoma cells via targeting acyl-CoA synthetase long-chain family member 1 (ACSL1) mRNA. Biochem Biophys Res Commun, 2014; 444: 270–75
36. Tang Y, Chen A: Curcumin protects hepatic stellate cells against leptin-induced activation *in vitro* by accumulating intracellular lipids. Endocrinology, 2010; 151: 4168–77

Indexed in: [Current Contents/Clinical Medicine] [SCI Expanded] [ISI Alerting System] [ISI Journals Master List] [Index Medicus/MEDLINE] [EMBASE/Excerpta Medica] [Chemical Abstracts/CAS] [Index Copernicus]